PROCEEDINGS OF SCIENCE

The Study of Extended Radio Galaxies in MERGHERS Fields

Banele Mthembu,[a,*] **Kenda Knowles**[b] **and Sinenhlahla Precious Sikhosana**[c]

[a] *School of Mathematics, Statistics and Computer Science, Astrophysics Research Center, University of KwaZulu-Natal, Durban, South Africa*

[b] *Department of Physics and Electronics, Rhodes University; South African Radio Astronomy Observatory (SARAO), Makhanda & Cape Town, South Africa*

[c] *School of Mathematics, Statistics and Computer Science, Astrophysics Research Center, University of KwaZulu-Natal (UKZN), Durban, South Africa*

E-mail: mphomthembu53@gmail.com, k.knowles@ru.ac.za, sikhosanap@ukzn.ac.za

We present a concise proceedings summary of our study of extended radio galaxies (ERGs) in the MeerKAT Exploration of Relics, Giant Halos, and Extragalactic Radio Sources (MERGHERS) Tier 1 field centred on ACT-CL J0438−5419 using MeerKAT L-band data at 1.28 GHz. Raw visibilities were processed with the *oxkat* pipeline through 1GC–3GC calibration and imaging, followed by primary-beam correction, astrometric checks, and sub-band imaging for in-band spectral index mapping. A cleaned catalogue of ERGs was assembled via *PyBDSF* and visual inspection. Cross-matching with RACS, SUMSS, and GLEAM-X provided broad-band fluxes; DECaLS and AllWISE enabled host identification and photometric redshifts. We report a morphology mix dominated by FRII sources, with FRI, WAT, HT, Z-shaped and unclassified sources also present. In-band spectral index maps show the expected steepening in outer lobes ($\alpha \lesssim -0.5$) and flatter spectra near cores, consistent with ongoing particle injection. We comment on environment for cluster vs field sources and outline future spectro-polarimetric extensions to the full MERGHERS sample.

High Energy Astrophysics in Southern Africa (HEASA2025)
16–20 September, 2025
University of Johannesburg, South Africa

*Speaker

 ISSN 1824-8039 . Published by SISSA Medialab.

PoS(HEASA2025)027

1. Introduction

Extended radio galaxies (ERGs) are active galaxies with large radio jets and lobes powered by accretion onto supermassive black holes. Their shapes and radio emission help us study jet physics, feedback, and how galaxies interact with their environment [3, 5, 15]. In practice, radio images and morphologies (e.g. FRI vs FRII) show where energy is injected and how jets interact with the surrounding gas [15]. Spectral index and curvature maps separate fresh particle acceleration from older plasma, giving rough ages and duty cycles for the sources [13]. On larger scales, radio power and lobe size relate to the mechanical work done on the hot gas, linking AGN jets to heating and feedback in clusters [5].

The MeerKAT telescope provides high sensitivity and resolution, making it ideal for detecting faint structures and studying spectral changes across extended sources. In this work, we present a small sample of ERGs in the MERGHERS [9] Tier 1 field centred on cluster ACT-CL J0438−5419. We briefly describe the data processing, catalogue creation, and initial science results, including morphologies, spectral index trends, and environments.

2. Data and Methods

2.1 Imaging and Calibration

We processed MeerKAT L-band data using the *oxkat* pipeline, including flagging, standard gain calibration (1GC–2GC), and direction-dependent calibration (3GC) with DDFacet+KillMS. After imaging, we applied primary beam correction and checked that the flux scale and astrometry were reliable by comparing compact sources with the RACS survey [12].

2.2 Astrometry and Flux Checks

We checked positional accuracy by matching MeerKAT sources with Gaia [2] and RACS. Small RA and Dec offsets were found and corrected. We also compared flux densities with RACS, scaling to 1.28 GHz for consistency, and found agreement within ~9.5%.

2.3 In-band Spectral Index Maps

We produced sub-band images centred roughly at 1.0, 1.2, and 1.4 GHz. These frequencies are approximate rather than exact because the effective centre of each sub-band depends on which channels were flagged during calibration and on the weighting applied during imaging. As a result, each sub-band represents an average frequency across the usable data. Spectral index maps created from these sub-bands help us trace energy losses in the radio plasma. Regions near the core show flatter spectra ($\alpha \gtrsim -0.5$) because the electrons there have been recently accelerated and still contain more high energy particles. As the plasma flows outward into the lobes, the electrons lose energy through synchrotron and inverse-Compton processes, which causes the spectra to steepen ($\alpha \lesssim -0.5$). In this way, the spectral index provides a simple indicator of where the jet is actively powered versus where the plasma is older and has been ageing.

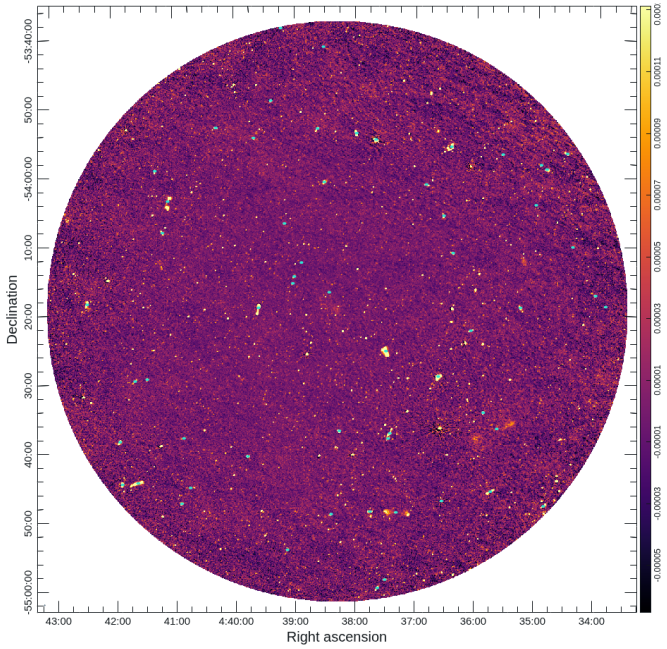

Figure 1: Primary beam-corrected MeerKAT image of the ACT-CL J0438−5419 field. Cyan circles mark the automated and visually confirmed ERGs.

2.4 Source Selection and Cross-Matching

Sources were first detected using *PyBDSF* and then visually inspected so that only extended radio galaxies were kept. We cross-matched our ERGs with several radio surveys: the Rapid ASKAP Continuum Survey (RACS; [12]), the Sydney University Molonglo Sky Survey (SUMSS; [11]), and the GLEAM-X survey from the MWA (GaLactic and Extragalactic All-sky MWA Survey–Extended; [8]). These surveys provide fluxes at lower frequencies, which help us calculate integrated spectral indices. We also matched our sources with optical data from the Dark Energy Camera Legacy Survey (DECaLS [1]) and with infrared data from the Wide-field Infrared Survey Explorer AllWISE release (AllWISE[2]) to identify host galaxies. Photometric redshifts were then estimated using the `zField` script from the `zCluster` [3] Python code. When redshifts were available, we used them to estimate the radio luminosities of the sources and Largest Linear Sizes (LLS).

3. Results

We identified 49 ERGs in the field. The sample contains several morphological types, dominated by FRII sources with some FRI, head–tail, wide–angle tail, Z-shaped, and unclassified sources.

[1] https://www.legacysurvey.org/
[2] https://irsa.ipac.caltech.edu/applications/wise/
[3] https://github.com/ACTCollaboration/zCluster

Table 1: The statistical results of the morphological classifications of sources in the ACT-CL J0438-5419 field.

Morphology	Number of sources	Fraction (%)
All	49	100.0
FRII	22	44.9
HT	6	12.2
Unclassified	13	26.5
FRI	3	6.0
WAT	4	8.2
Z-shape	1	2.0

3.1 Spectral Index

The spectral index α describes how the radio flux density changes with frequency, and is defined by the power-law relation

$$S_\nu \propto \nu^{-\alpha},$$

where S_ν is the flux density at frequency ν. A flatter spectral index (typically $\alpha \gtrsim -0.5$) is found near radio cores and hotspots, where fresh, high-energy particles are being injected by the central engine. Steeper values ($\alpha \lesssim -0.5$) occur in the outer lobes, where the plasma has aged, and high energy electrons have lost energy through synchrotron radiation (see Figure 2) [10, 14]. Thus, the spectral index provides a simple way to trace regions of active jet powering versus older, radiatively cooled emission.

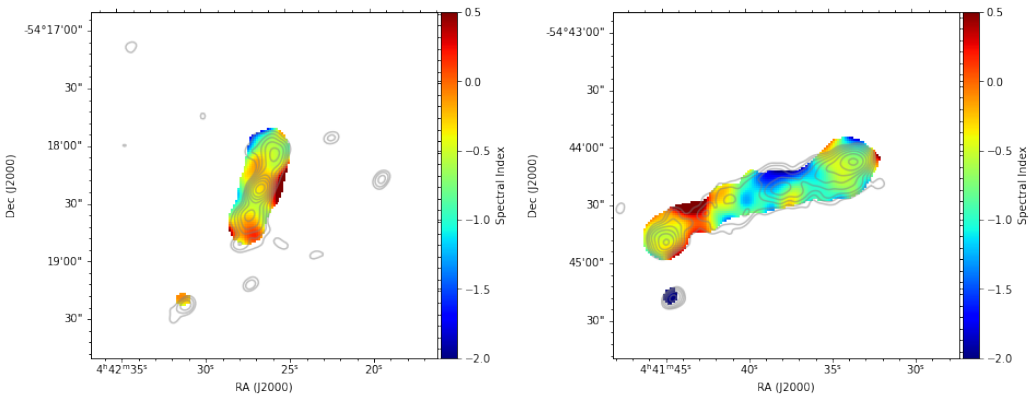

Figure 2: In-band spectral index maps of selected radio sources from MeerKAT L-band observations, showing data across three observed frequencies: 1.0, 1.2, and 1.4 GHz. Shown in gray are the overlaid contours of the corresponding L-band map. The contours were generated at levels of 3σ and increase in steps 3σ, where σ is the local rms noise which is 12.1 µJy/beam.

4. Environment

Bent radio galaxies such as wide-angle tail (WAT) and head–tail (HT) sources are often linked to dense cluster environments, where the jets interact with the hot intracluster medium (ICM) [15]. We

see similar behaviour in our field. In contrast, most FRII galaxies appear to lie in lower density or field environments where their jets can expand with fewer disturbances, consistent with previous studies [1].

To determine whether a source was associated with a known cluster, we first tested whether any ERGs lay within the estimated R_{200} radius of ACT-CL J0438−5419 field, using M_{200} values from the literature to compute R_{200}. No source in our sample fell within this cluster radius. We then used the positions of ERGs with available photometric redshifts and performed a 10 arcminute radius search in SIMBAD[4] to check for proximity to any catalogued clusters. This radius search window was chosen to allow for typical positional uncertainties and to capture sources that may be spatially linked to a cluster environment. Based on this approach, we found that 6 sources (33.3%) are consistent with being associated with a known cluster. These include three FRIs, two WATs, and one Z-shaped radio galaxy. The remaining host-identified sources with redshifts (11/17) showed no association with any catalogued cluster and are therefore classified as *field* sources. Most of these field systems are classical FRIIs, with well-collimated jets ending in compact hotspots and smooth emission between the core and lobes. Figure 3 illustrates examples of ERGs in both cluster and field environments.

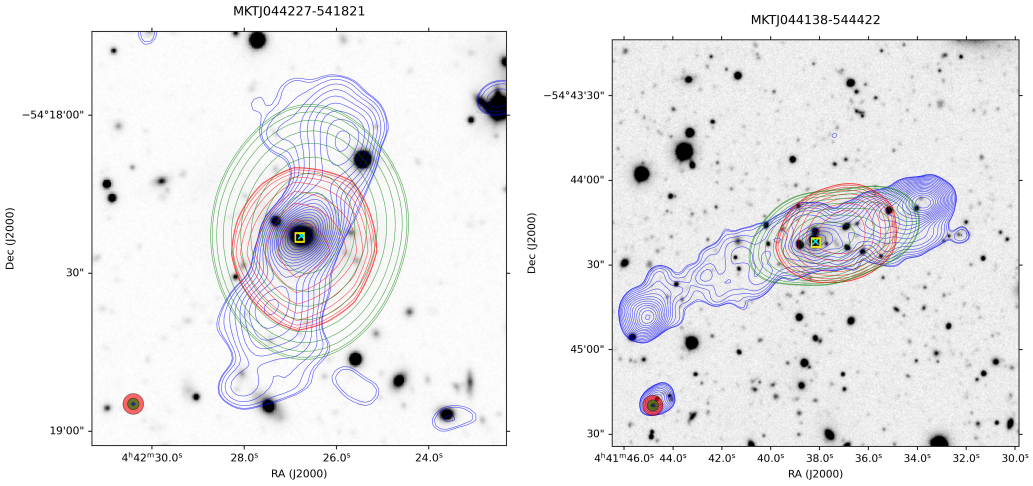

Figure 3: An overlay of radio sources with FRI **(Left image)** and FRII **(Right image)** morphology from the MeerKAT sample. The radio contours are from MeerKAT L-band observations (856 − 1712 MHz; blue) with a resolution of $\sim 8.2''$, SUMSS (843 MHz; red), and RACS (888 − 1032 MHz; green), overlaid on the inverted grayscale DECaLS image. The bottom-left corner shows the beam sizes: MeerKAT (blue), SUMSS (red), and RACS (green). Cyan cross = host galaxy; yellow square = *PyBDSF* radio position.

5. Conclusions

We present here two examples of extended radio galaxies in the MERGHERS for the ACT-CL J0438−5419 field observed with MeerKAT L-band. Our main findings are FRII sources dominate the sample, with several bent-tail systems. In-band spectral index maps show expected ageing patterns.

[4] https://simbad.cds.unistra.fr/simbad/

For the radio sources shown in Figure 2, we present here two examples that display particularly interesting spectral features, selected from the 49 sources in our sample. The in-band spectral index maps in Figure 2 for the two selected radio sources, shows a steepening of the spectrum toward the outer edges of both lobes, with $\alpha \lesssim -0.5$. This agrees with synchrotron aging, where particles lose energy as they move away from the central core [6]. Closer to the core and hotspot regions, flatter indices are observed ($\alpha \gtrsim -0.5$), which is characteristic of regions where active jet material is being injected.

Our environmental analysis shows that FRI and WAT systems are more commonly found in clusters, where the dense intracluster medium influences their jet structures. In contrast, most FRII sources in our redshift-identified subsample lie in the field, consistent with previous studies that associate them with lower density environments. Interestingly, we also found two HT sources and one WAT source in the field, which is less common, but similar cases have been reported in the literature [16]. For the contour overlays depicted in Figure 3, the image on the left exhibit FRI morphology. The MeerKAT contours reveal diffuse, elongated emission extending symmetrically from the central core, which coincides with the cyan host galaxy. The lobes display a darkened edge structure, and we observe a diffuse and gradual decrease in brightness as they extend outwards, a characteristic feature of FRI galaxies [4]. The image on the right depicts two bright lobes on opposite sides, both clearly connected to the central core, which is typical for an FRII radio galaxy. The blue contours from MeerKAT show well-defined lobes extending from the center, matching the expected morphology of an FRII source [7].

Future work will include spectro-polarimetric analysis, improved redshift estimates, and extending this study to all MERGHERS fields.

Acknowledgments

We acknowledge the opportunities to present parts of this work at various conferences, including SARAO, Cosmology on safari, and HEASA. We acknowledge the ilifu supercomputer, which made the data processing and analysis in this research possible. we also acknowledge NASSP support.

References

[1] Capetti, A., Massaro, F., and Baldi, R. D. (2017). Friicat: a first catalog of fr ii radio galaxies. *Astronomy & Astrophysics*, 601:A81.

[2] Collaboration, G. et al. (2018). Vizier online data catalog: Gaia dr2 (gaia collaboration, 2018). *VizieR Online Data Catalog*.

[3] Fanaroff, B. L. and Riley, J. M. (1974). The morphology of extragalactic radio sources of high and low luminosity. *Monthly Notices of the Royal Astronomical Society*, 167:31P–36P.

[4] Hardcastle, J. M. (2005). Jets, hotspots and lobes: what x-ray observations tell us about extragalactic radio sources.

[5] Hardcastle, M. J. and Croston, J. H. (2018). Radio galaxies and feedback from agn jets. *New Astronomy Reviews*, 91:81–139.

[6] Harwood, J. J., Hardcastle, M. J., Croston, J. H., and Goodger, J. L. (2013). Spectral ageing in the lobes of fr-ii radio galaxies: new methods of analysis for broad-band radio data. *Monthly Notices of the Royal Astronomical Society*, 435(4):3353–3375.

[7] Hesterly, K. L. (2021). *High-Resolution Maps of FRII DRAGNs*. The University of Manchester (United Kingdom).

[8] Hurley-Walker, N., Galvin, T. J., Duchesne, S. W., Zhang, X., Morgan, J., Hancock, P. J., An, T., Franzen, T. M. O., Heald, G., Ross, K., Seymour, N., Veenboer, B., Williams, W. L., Callingham, J. R., Johnston-Hollitt, M., Line, J. L. B., McKinley, B., Staveley-Smith, L., and Webster, R. (2022). The galactic and extragalactic all-sky mwa survey – extended (gleam-x) i: Survey description and initial data release. *Publications of the Astronomical Society of Australia*, 39:e035.

[9] Knowles, K., Intema, H. T., Baker, A. J., Bharadwaj, V., Bond, J. R., Cress, C., Gupta, N., Hajian, A., Hilton, M., Hincks, A. D., Hlozek, R., Hughes, J. P., Lindner, R. R., Marriage, T. A., Menanteau, F., Moodley, K., Niemack, M. D., Reese, E. D., Sievers, J., Sifón, C., Srianand, R., and Wollack, E. J. (2016). MeerKAT Science: On the Pathway to the SKA. *Monthly Notices of the Royal Astronomical Society*, 459.

[10] Mahatma, V. H., Hardcastle, M. J., Croston, J. H., Harwood, J., Ineson, J., and Moldon, J. (2020). Investigating the spectral age problem with powerful radio galaxies. *Monthly Notices of the Royal Astronomical Society*, 491(4):5015–5034.

[11] Mauch, T., Murphy, T., Buttery, H. J., Curran, J., Hunstead, R. W., Piestrzynska, B., Robertson, J. G., and Sadler, E. M. (2008). The sydney university molonglo sky survey (sumss) – version 2.1 catalogue. *VizieR Online Data Catalog*, 8081. II/281.

[12] McConnell, D., Hale, C. L., Lenc, E., and et al. (2020). The rapid askap continuum survey i: Design and first results. *Publications of the Astronomical Society of Australia*, 37:e048.

[13] Miley, G. K. (1980). The structure of extended extragalactic radio sources. *Annual Review of Astronomy and Astrophysics*, 18:165–218.

[14] Murgia, M., Fanti, C., Fanti, R., Gregorini, L., Klein, U., Mack, K.-H., and Vigotti, M. (2002). Synchrotron spectra and ages of compact steep spectrum radio sources. *New Astronomy Reviews*, 46(2-7):307–311.

[15] Owen, F. N. and Ledlow, M. J. (1997). The Fanaroff-Riley transition and the distribution of radio galaxies in the abell cluster environment. *Astrophysical Journal Supplement Series*, 108:41–56.

[16] Pal, S. and Kumari, S. (2023). A new catalog of head–tail radio galaxies from LoTSS DR1. *Journal of Astrophysics and Astronomy*, 44(17).